

# Image Fusion for Computer-assisted Bone Tumor Surgery

Kwok Chuen Wong MD, Shekhar Madhuker Kumta MD,  
Gregory Ernest Antonio MD, Lung Fung Tse MD

Received: 21 January 2008 / Accepted: 20 June 2008 / Published online: 22 July 2008  
© The Association of Bone and Joint Surgeons 2008

**Abstract** The fusion of computed tomography and magnetic resonance images is a software-dependent processing technique that enables one to integrate and analyze preoperative images for planning complex musculoskeletal tumor resections. By integrating various imaging modalities into one imaging data set we may facilitate preoperative image analysis and planning of navigation computer-assisted bone tumor resection and reconstruction. We performed image fusion for computer-assisted tumor surgery in 13 consecutive patients, seven males and six females, with a mean age of 35.8 years (range, 6–80 years). Visual verification of fused images was accurate in all patients. The mean time for image fusion was 30.6 minutes (range, 8–80 minutes). After intraoperative registration, all tumor resections were performed as planned preoperatively under navigation image guidance.

Each author certifies that he or she has no commercial associations (eg, consultancies, stock ownership, equity interest, patent/licensing arrangements, etc) that might pose a conflict of interest in connection with the submitted article.

Each author certifies that his or her institution has approved the human protocol for this investigation, that all investigations were conducted in conformity with ethical principles of research.

**Electronic supplementary material** The online version of this article (doi:10.1007/s11999-008-0374-5) contains supplementary material, which is available to authorized users.

K. C. Wong (✉), S. M. Kumta, L. F. Tse  
Department of Orthopaedics and Traumatology, The Chinese University of Hong Kong, Prince of Wales Hospital, Shatin, Hong Kong  
e-mail: skcwong@ort.cuhk.edu.hk

G. E. Antonio  
Department of Diagnostic Radiology and Organ Imaging, The Chinese University of Hong Kong, Prince of Wales Hospital, Shatin, Hong Kong

Resections achieved after navigation resection planning were validated by postoperative CT or resected specimens in seven patients. Histologic examination of all resected specimens showed tumor-free margins in patients with bone sarcoma. The fusion of computed tomography and magnetic resonance imaging has the potential to enhance computer-assisted bone tumor surgery. The fusion image, when combined with surgical navigation, helps surgeons reproduce a preoperative plan reliably and may offer substantial clinical benefits.

**Level of Evidence:** Level IV, therapeutic study. See the Guidelines for Authors for a complete description of levels of evidence.

## Introduction

Computer-assisted intraoperative navigation has been used effectively in orthopaedic trauma, spinal, and joint replacement surgery [1, 3, 4, 8, 16], but has not been used extensively in musculoskeletal bone tumor surgery [6, 7]. Computed tomography (CT)-based navigation for pelvic tumor resection and reconstruction with a custom pelvic prosthesis was reported to be successful [18].

Computed tomography and MRI are essential preoperative studies before complex bone tumor surgery. Computed tomography scans show intricate bony details well, whereas MRI is superior in delineating the intraosseous and extraosseous extensions of tumor, particularly in soft tissues and in relation to regional anatomy. Fusion of CT and MRI yields hybrid images that combine the key characteristics of each technique, thus enabling better interpretation of each and accurate localization of the lesion. This image processing technique has been used in navigation-assisted neurosurgical and otorhinolaryngeal

procedures [9, 12], but has not been widely used in musculoskeletal tumor surgery [17].

We investigated the possibility of fusing multimodal preoperative imaging studies, using a proprietary surgical navigation software for three-dimensional (3-D) surgical planning for resection of musculoskeletal bone tumors. We also examined whether the image-fusion technique allowed us to reproduce the surgical plan reliably and accurately by evaluating the: (1) accuracy of the image fusion and preoperative time to achieve it; (2) accuracy as determined by comparing the resection with the preoperative surgical plan, assessing the margins of the resected tumor specimens, and assessing the fit of the custom tumor prostheses to the remaining bone; (3) additional time needed for navigation procedures at the time of surgery and complications of the procedures; and (4) accuracy of the image-to-patient registration.

## Materials and Methods

We studied 13 patients (seven males, six females), between 6 and 80 years (mean, 35.8 years) of age, with tumors located in the pelvis ( $n = 2$ ), sacrum ( $n = 6$ ), femur ( $n = 4$ ), and proximal tibia ( $n = 1$ ) (Table 1). Tumor types included osteosarcoma (four), chordoma (two), chondrosarcoma (one), undifferentiated bone sarcoma (one), metastatic uterine carcinoma (one), malignant peripheral nerve sheath tumor (one), sacral schwannoma (one), and giant cell tumor of bone (one). We judged computer-assisted surgery important in these patients because of the complex anatomy of the affected bone (pelvis, sacrum), the need for precision in joint-saving intercalated resections where custom prostheses were used for reconstruction, or because of severe scarring resulting from previous surgery and radiotherapy.

Axial CT images of the lesion and surrounding area were acquired using a 16-detector scanner (General Electric Light Speed, Milwaukee, WI). Slices with 0.625-mm or 1.25-mm thickness were obtained using a soft tissue algorithm. Magnetic resonance images of the corresponding region were acquired using a 1.5-T unit (Siemens Sonata, Erlangen, Germany). For Patients 1 through 8, postcontrast T1-weighted axial images (TR 512 ms, TE 13 ms, 2-mm thick slices) were used for fusion with CT images because of better bone-soft tissue contrast. For Patients 1 through 8, image data sets were imported into a navigation system (Stryker Navigation, Freiburg, Germany; CT spine, version 1.6) for image fusion. For Patients 9 through 13, an upgraded version of the software for cranial navigation (Stryker Navigation; iNtellect Cranial, version 1.1) allowed us to use MR image sequences regardless of scan orientation.

For the CT spine navigation software, image fusion involved cross-sectional matching of the anatomic structures on the CT with those on the MR image—a process called “coregistration.” The system allowed CT and MR images to be fused by matching the manually segmented known structures in corresponding CT and MRI data sets.

In the latter part of the study, the cranial navigation software allowed automatic fusion of various image data sets regardless of imaging modalities and scan orientation. Final fused images also could be adjusted manually in different dimensions to improve accuracy. The system allowed viewing the fusion image in the splitting mode and fusion mode (Fig. 1). In the splitting mode, the active window was divided into two parts, each of which displayed the images of selected modality (Fig. 1C). In the fusion mode, a new image was calculated as the weighted sum of the base and overlay images (Fig. 1A, B). The weighting was defined with a slider bar. Dragging the slider to either series of fusion image allowed us toggle between the image series thereby making it possible to vary the predominance of a particular modality where this toggle feature may be seen. (Supplementary videos 1, 2, and 3 are available with the online version of CORR.) We considered the fusion image acceptable for navigation planning if the bony contours on the CT/MR images at the region of interest matched within a 1-mm margin of error as visually assessed by the authors. The data sets of the fused images then were transferred back to the navigation system (CT spine navigation software) for resection planning.

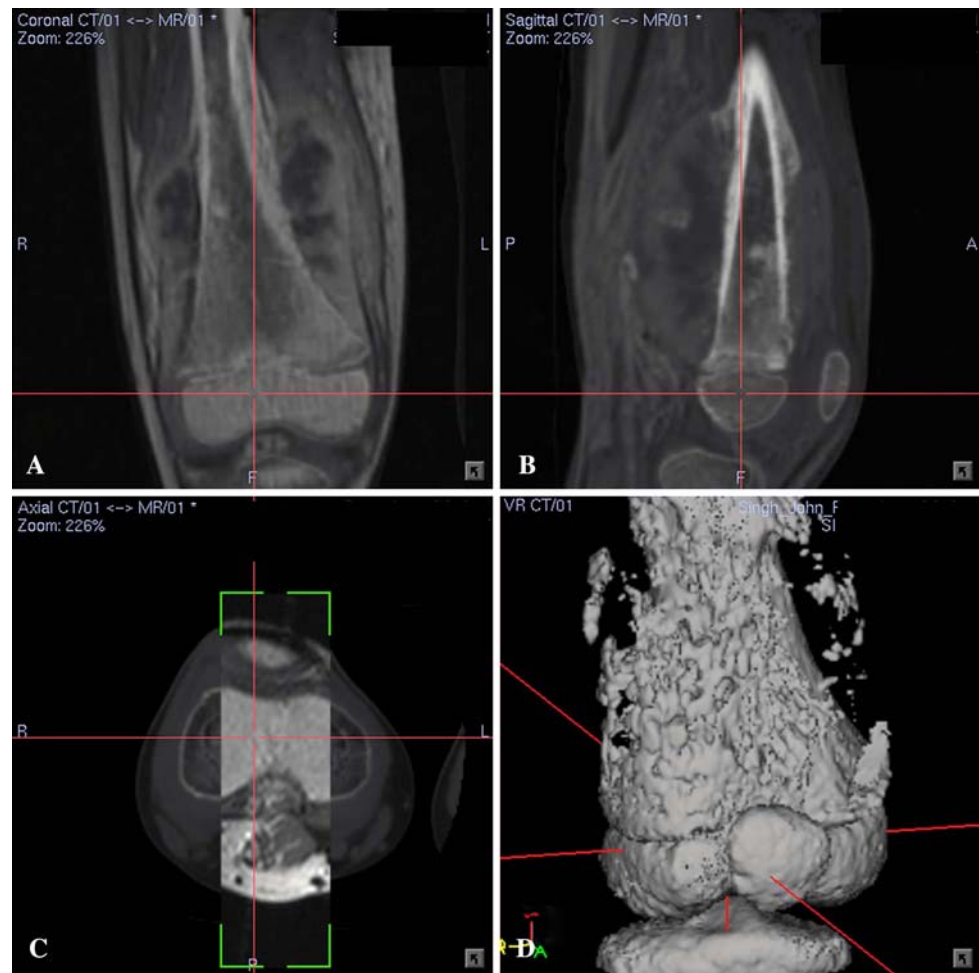
We began navigation planning by defining the extent of the tumor, followed by segmenting the tumor volume from the MR images. We determined the tumor edge by looking at the transition of marrow signal from abnormal to normal in T1-weighted MR images. Areas of intermediate signal intensity adjacent to tumor edge that might represent microscopic metastases or marrow hyperplasia were regarded as being part of the tumor. We then created a 3-D bone model by adjusting the contrast of the CT images. As CT/MR images share identical spatial coordinates after image fusion, segmented tumor volume obtained from MR images was incorporated directly into the reconstructed 3-D bone model. A 3-D bone tumor model was generated. The anatomic extent of the tumor and its relationship with the surrounding structures were studied by blending 2-D pure CT, pure MR images, and fusion images and observing the 3-D bone tumor model from different directions and magnifications on the navigation display. (Supplementary videos 1, 2, and 3 are available with the online version of CORR.) The planned margin of local resection ranged from 0.5 cm to 2 cm from the tumor edge and depended on whether the patient had bone metastases, primary bone sarcoma, and whether any neoadjuvant therapy was given. Marginal excision was planned for the

**Table 1.** Demographic data for 13 patients

Patient number	Age (years)	Gender	Diagnosis	Location	Surgery	Bone reconstruction	Preoperative fusion imaging data sets	Fusion time (minutes)	Navigation planning time (hours)	Navigation time (minutes)	Function (MSTS score*)	Followup (months)
1	46	F	Parosteal osteosarcoma	Left proximal tibia (posterior aspect)	Joint-saving resection	Vascularized fibular graft	CT angiogram and MRI of proximal tibia	60	2	40	28	19
2	42	F	Metastatic uterine carcinoma	Left ischial tuberosity	Local resection	No	CT and MRI of pelvis	40	0.75	13	—	18
3	24	F	Undifferentiated bone sarcoma	Right proximal femur	Local resection after neoadjuvant chemotherapy	Modular tumor prosthesis	CT and MRI of proximal femur	60	1.5	18	29	17
4	53	F	Schwannoma	Right S2 nerve root	Excision through posterior approach	No	CT of pelvis and MRI of sacrum	30	1.0	15	—	13
5	14	M	Conventional osteosarcoma	Right femur (from sub-trochanteric region to distal physis)	Joint-saving resection after neoadjuvant chemotherapy	Custom tumor prosthesis <sup>†</sup>	CT of femur and MRI of proximal femur; CT of femur and MRI of distal femur <sup>§</sup>	80	2.5	30	29	12
6	80	F	Chordoma	Sacrum (below and including S2)	Resection	No	CT of pelvis and MRI of sacrum	40	1.5	35	—	11
7	6	M	Conventional osteosarcoma	Right distal femur	Joint-saving resection after neoadjuvant chemotherapy	Custom tumor prosthesis <sup>†</sup>	CT of femur and MRI of distal femur	30	2.0	20	26	7
8	54	M	Giant cell tumor	Sacrum (from S1 to S4)	Intralesional curettage through posterior approach	No	CT angiogram and MRI of pelvis	40	1.5	25	—	6
9	8	M	Conventional osteosarcoma	Left distal femur	Joint-saving resection after neoadjuvant chemotherapy	Custom tumor prosthesis <sup>†</sup>	CT and MRI of distal femur	10	1.0	15	29	5
10	50	M	Recurrent chordoma	Left pelvic metastases	Resection (PII)	Custom tumor prosthesis <sup>†</sup>	CT angiogram, MRI, and PET of pelvis	20	1.5	15	25	4
11	18	M	Conventional osteosarcoma	Sacrum (from S1 to S5)	Total sacrectomy	No	CT and MRI of pelvis	8	1.0	15	—	4
12	54	F	Recurrent chondrosarcoma	Sacrum (from S1 to S5)	Total sacrectomy	No	CT angiogram and MRI of pelvis	10	1.0	25	—	4
13	17	M	Recurrent malignant nerve sheath tumor	Left sciatic nerve and involving ilium and sacrum	Left extended hemipelvectomy (resection through sacral alar and neural foramina)	No	CT angiogram, MRI, and PET of pelvis	20	1.5	30	—	3

\*MSTS = Musculoskeletal Tumor Society score; <sup>†</sup>custom-made prosthesis was a computer-aided design based on preoperative CT images of patients and information from navigation planning; <sup>§</sup>Patient 5 with extensive tumor involvement, separate MR images of the distal femur and proximal femur were fused on one CT image of the whole femur for planning of distal and proximal femur resection because it was impossible to take a good-quality MR image of the whole femur with 2 mm thickness for image fusion; CT = computed tomography; PET = positron emission tomography.

**Fig. 1A–D** (A) Coronal and (B) sagittal sections of CT/MR fusion images for Patient 7 with a right distal femur osteosarcoma are shown. The fusion images were in the fusion mode which had slightly higher CT weighting than MR images. (C) The cross section of the CT/MR fusion image was made in the splitting mode in which the rectangular window displayed overlay MR images on the base CT images. The image fusion was accurate and acceptable for navigation planning if the bony contours on CT/MR images at the region of interest matched within a 1-mm margin of error as visually assessed by the authors. (D) The 3-D bone model reconstructed from CT images is shown.



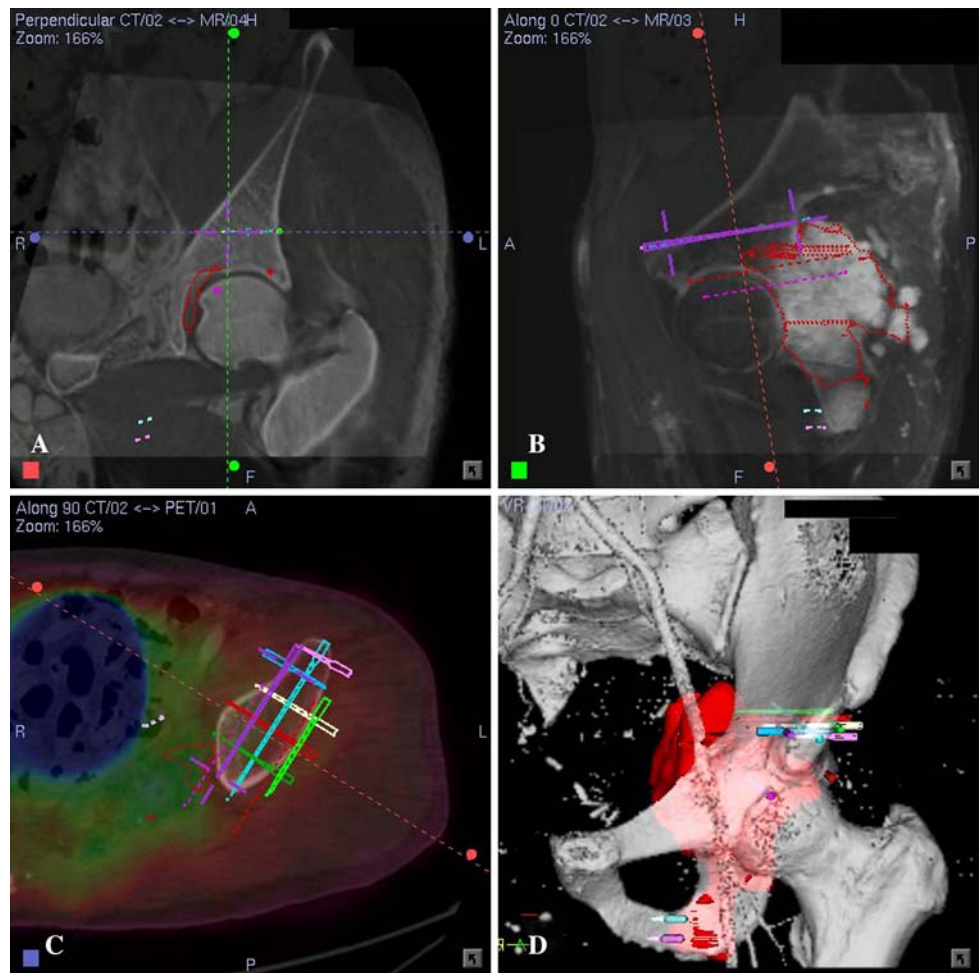
sacral schwannoma in Patient 4, whereas intralesional excision was planned for the sacral giant cell tumor in Patient 8. We then placed virtual markers (pedicle screws in CT spine navigation software) along the plane and orientation of the planned tumor resection. In Patients 5, 7, 9, and 10, the computer-aided design data of the custom-made prostheses provided by the manufacturer (Stanmore Implants Worldwide Limited, Middlesex, UK) also were integrated in the navigation resection planning (Fig. 2). To evaluate whether fusion images were valuable for surgical planning in a CT-based navigation system, we compared resection planning using only CT or MR images with resection using fused images. Fusion images were considered valuable if additional information not seen on conventional images was obtained for resection planning.

Intraoperative navigation has been described [17, 18]. The image-to-patient registration to match the corresponding points between the patient's real intraoperative anatomy and preoperative CT images was performed by paired points and surface matching. The navigation system calculated the registration error which indicated the degree of mismatch, if any, between preoperative CT images and

the patients' anatomy. We then assessed real-time matching between the anatomy and the virtual images by running the registration probe on the bone surface and by checking specific known and well-defined anatomic landmarks. The navigation system was considered accurate only if there was exact matching between the image on the navigation console and the patient's skeletal anatomy. Soft tissues around the bone tumor might deform after surgical exposure, resulting in discrepancies between preoperative anatomic data and real-time surgical anatomy. Therefore, we could use this technique only to guide the resection of a bone as bony anatomy does not change after surgical exposure. Intraoperative navigation then was performed on CT/MR fusion images and the 3-D bone tumor planning model. The fusion images were manipulated to highlight CT or MRI features (Fig. 3). We next located the anatomic position of virtual markers (pedicle screws) on our patients, using navigated tools, and marked the intended resection by diathermy or drill. The diathermy or drill marks were connected to form the final resection level and plane. The tumor was removed en bloc by an oscillating saw or osteotome.



**Fig. 2A–D** (A) A coronal section of the CT/MR fusion image for Patient 10 with left pelvic metastases from a previously treated sacral chordoma is shown. The central cross represented the virtual marker (pedicle screw in CT spine navigation software) that marked the level and orientation of bone resection above the hip. (B) The CT/MR fusion image along the direction of the virtual screw marking the resection level and orientation is shown. (C) A cross section of the CT/PET fusion image at the resection level above the hip is shown. Lack of uptake on the PET images at the planned resection level helped determine the tumor-free bone resection. Level and orientation of resection above the hip was defined precisely with the help of virtual screws that were based on computer-aided design data of a custom-made pelvic prosthesis. (D) A 3-D bone tumor model reconstructed from the CT angiogram and MR image data sets is shown. Virtual screws marked the bone resection above the hip and at the inferior pubic rami.



We recorded the following variables: (1) accuracy and time required for image fusion and navigation planning; (2) intraoperative error of image-to-patient registration; (3) histologic evaluation of resection margins in all tumor specimens (except those of Patient 4 with a sacral schwannoma and Patient 8 with a sacral giant cell tumor as both underwent marginal or intralesional excisions of their tumors); and (4) matching between residual bone and custom prosthesis junction at the surgery. To validate whether the resection achieved was the same as planned, CT images of the resected specimen for Patient 3 and postoperative CT images of the pelvis for Patients 2 and 6 were obtained and fused with preoperative CT images. The cross sections at the resection plane of the resected specimens for Patient 5, 7, 8, 10 were measured and compared with their preoperative navigation plans. The resection achieved was considered the same as planned if the matching was within 1 mm difference. We did not validate the resections for Patients 4 and 8 with benign tumors (marginal/intralesional excision) and Patients 1, 11, 12, and 13 as their resection planes were irregular and curved. Functional assessment was performed using the

Musculoskeletal Tumor Society (MSTS) score [2] in patients with limb salvage surgery.

## Results

Image fusion was feasible for all patients with tumors at different regions. We judged the fusion images accurate and acceptable for navigation planning in the areas of clinical interest as the bony contours of the CT/MR fusion images matched to within 1 mm difference. By combining the bony information of CT, soft tissue contrast of MRI, and metabolic information of positron emission tomography (PET) (Patients 10 and 15) in one image, we found it easier to distinguish between normal and pathologic structures (Fig. 4). (Supplemental video 3 is available with the online version of CORR.)

The resection achieved, in terms of dimensions and orientation, was as planned in the seven patients whose resections were validated either by fusing postoperative with preoperative CT images or comparing the resection plane of resected specimens with that in surgical navigation

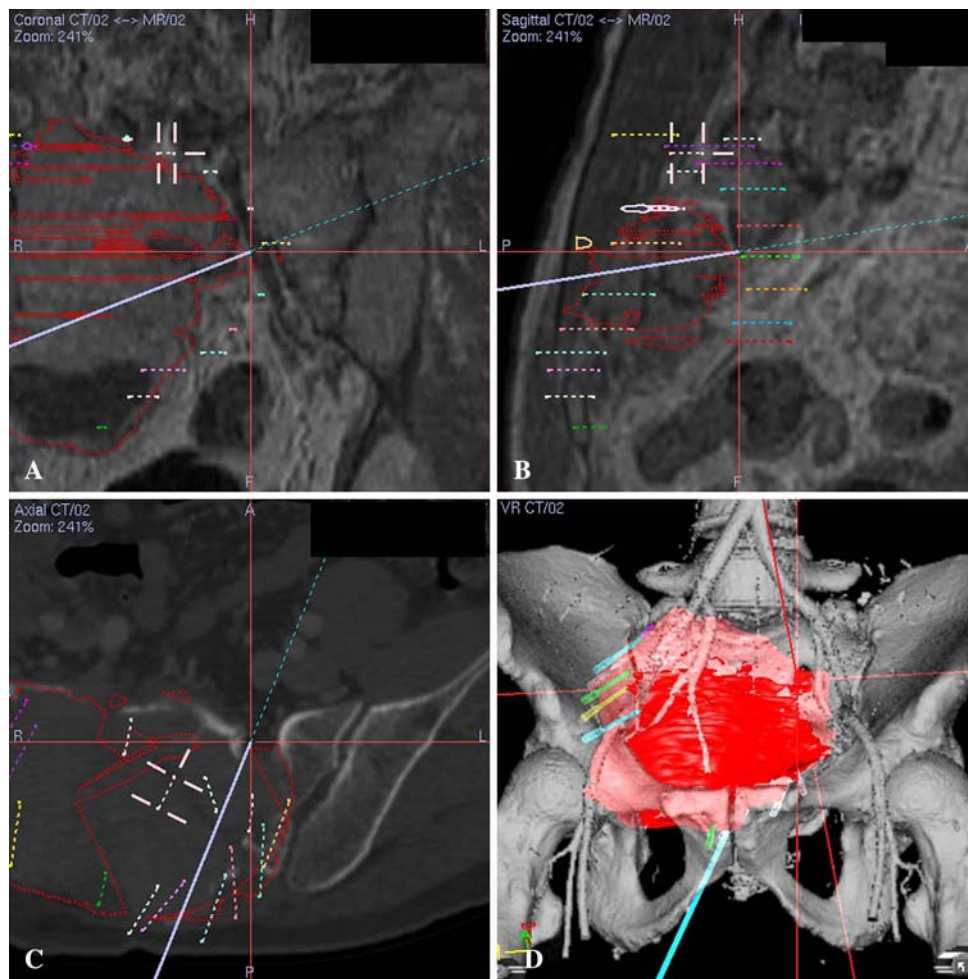


**Fig. 3A–D** (A) A coronal section of the CT/MR images at surgery (intralesional curettage via a posterior approach) for Patient 8 with a sacral giant cell tumor was made in the fusion mode with more MR weighting than CT images to facilitate visualization of soft tissue. Intralesional curettage still necessitated direct vision at the tumor cavity. However, surgeons had better understanding of the distorted anatomy of the anterior bony structure of the sacrum by correlating with preoperative imaging under navigation guidance. The purple line represents the direction of the navigated bone burr and its tip at the center of the red cross points to the left anterior S1 foramen with the associated S1 nerve root. (B) A sagittal section of the CT/MR images obtained at the time of

surgery was made in the fusion mode with more MRI weighting than CT images. The cross represents the tip of the navigation probe that points to the left S1 foramen. (C) A cross section of pure CT images shows the bony structure of the sacral tumor at surgery. (D) A 3-D bone tumor model was reconstructed from the CT angiogram and MR image data sets. Branches from the right internal iliac artery were displaced anteriorly by the tumor mass. The 3-D and various 2-D fusion images helped surgeons orientate the complex and distorted anatomy and maximally preserve normal bone by making a precise posterior cortical window adequate for intralesional tumor curettage. The virtual screws marked the extent of the posterior cortical window.

planning. Histologic examinations of all specimens showed a clear tumor margin in patients with malignant bone tumors. We found a match between residual bone and custom prosthesis junction in four patients at surgery.

With the CT spine navigation software (Patients 1 through 8), the mean time for image fusion was 47.5 minutes (range, 30–80 minutes), whereas it was 13.6 minutes (range, 8–20 minutes) when the newer cranial navigation software was used (Patients 9 through 13). The mean time for preoperative navigation planning after image fusion in CT spine navigation software was 1.4 hours (range, 0.75–2.5 hours). The planning time depended on case complexity.

The mean intraoperative accuracy of image-to-patient registration was 0.46 mm (range, 0.35–0.68 mm). The virtual preoperative CT images correlated well with the patients' anatomy after registration. All surgeries were performed as planned under navigation guidance after registration. The mean time for navigation procedures during surgery was 24.3 minutes (range, 13–40 minutes).

A postoperative superficial wound infection developed in one patient (Patient 6 with a sacral chordoma) that resolved with administration of an intravenous antibiotic, whereas a wound infection in another patient (Patient 11 with a sacral osteosarcoma) required surgical debridement and antibiotics. No patients experienced local recurrence at

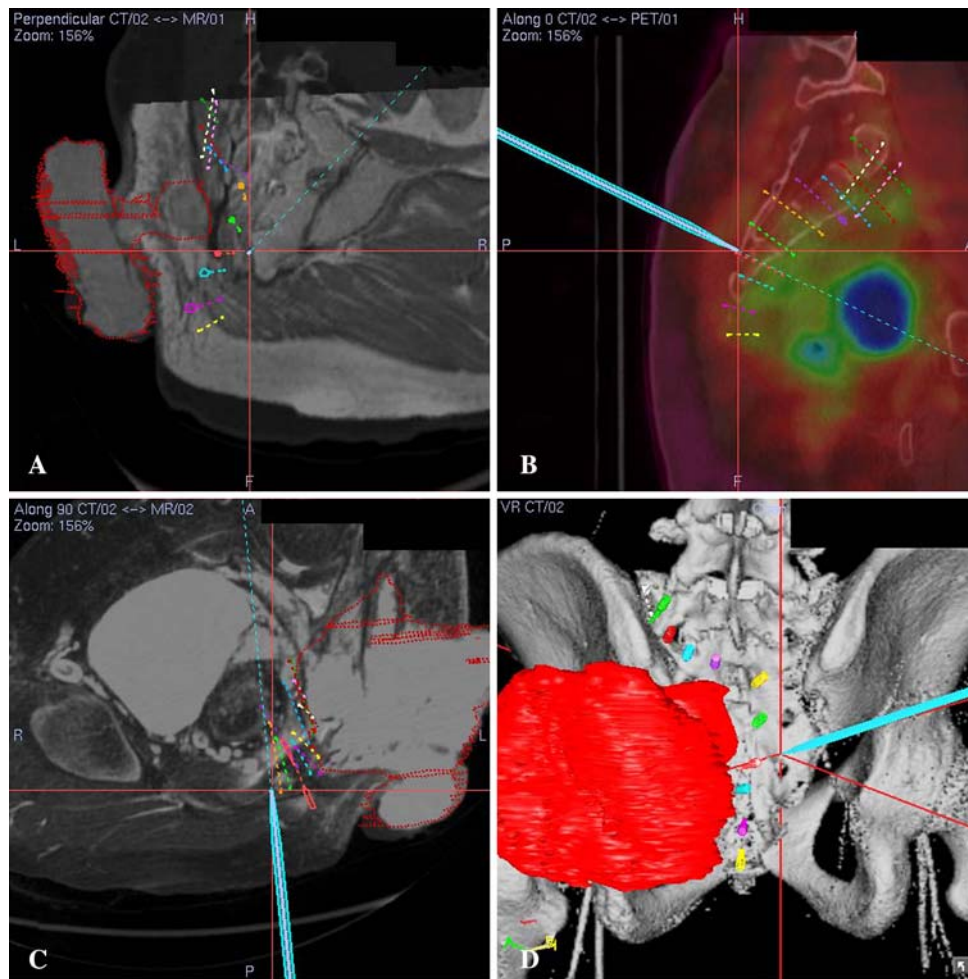


**Fig. 4A–D** (A) An oblique view of the CT/MR fusion image obtained at surgery for Patient 13 with a recurrent buttock sarcoma after two previous operations and radiotherapy is shown. The cross represents the tip of the navigation probe on the posterior sacral bone surface. (B) A sagittal view of the CT/PET fusion image obtained at surgery is shown. PET images were useful to differentiate active tumor from scar tissue and thus provide additional information for determination of actual tumor volume segmented initially from MR image datasets. (C) A cross section of the CT/MR fusion image

obtained at surgery and (D) a 3-D bone tumor model reconstructed from the CT angiogram and MR image data sets are shown. The tumor (red) arose from the sciatic nerve at the greater sciatic notch and invaded the sacroiliac joint and lateral part of the sacrum. The virtual screws marked the path of sacral resection. The navigation probe (light green) touched the posterior sacral bone surface near the left S4 posterior neural foramen. Corresponding 2-D views are shown on these illustrations. (Supplemental video 3 is available with the online version of CORR.)

a minimum followup of 3 months (mean, 9.5 months; range, 3–19 months). The mean functional MSTS score for patients with limb salvage surgery was 27.7 of 30 (range, 25–29).

## Discussion

To achieve safe tumor resections, one must observe the extent of the tumor in the bone and soft tissues. Computed tomography and MRI are preoperative investigations necessary for planning complex musculoskeletal bone tumor resections and reconstructions. Computed tomography and MRI provide information that is represented in a 2-D

imaging format. Tumor surgeons must mentally integrate this 2-D information into a 3-D model for surgical planning. The difficulty of this mental integration increases with the complexity of the regional anatomy. We evaluated the (1) accuracy of image fusion and preoperative time to achieve it; (2) accuracy as determined by comparing the resection with the preoperative surgical plan, assessing the margins of the resected tumor specimens, and assessing the fit of the custom tumor prostheses to the remaining bone; (3) additional time needed for navigation procedures at the time of surgery and complications of the procedures; and (4) accuracy of the image-to-patient registration.

Our study has important limitations. Although histologic examination of all specimens with bone sarcoma showed a



clear tumor margin, margins alone are not the only determinants of good clinical results in terms of better survival or reduced local recurrence; further, a judgment of clear margins is based upon a small sampling of the entire margin. Our series is heterogeneous in diagnosis and lacks a control group; therefore, it is not possible to make a comparative assessment of clinical results. Long-term followup in a larger series is needed to evaluate the clinical importance of the technique. However, we presume if surgical planning can be reproduced accurately and reliably, the chances of a good clinical result are likely to be greater. The technique requires surgeons who have prior experience in navigation surgery and additional resources for navigation facilities. Therefore, we used navigation only for patients in whom tumor resection was expected to be complicated owing to anatomic reasons or scarring, or for patients in whom the complexity of resection demanded customized prostheses that could be fitted into the defect only if the precise amount of bone was resected.

Image fusion technology has been used successfully in complex lesions at the head and neck regions [9, 12]. Incorporation of this technology has enhanced the capacity of surgical navigation, especially for skull base surgery. Our experience shows fusion images could be feasible and accurate in other complex regions such as the pelvis and sacrum. Navigation software allowed us to scrutinize all fused image data sets in three spatial dimensions in a short time. An additional fourth dimension of image analysis was possible by continuous blending of CT and MRI data, thus providing an excellent mental picture of anatomic tumor location and extent of infiltration into surrounding tissues. Image fusion might not be restricted to plain CT or MRI data sets. The CT angiogram and MRI fusion (Patients 1, 8, 10, 12, 13) provided key additional information regarding regional vascular anatomy that facilitated preoperative planning. Functional imaging such as F-18 fluorodeoxyglucose PET scans also could be incorporated into the navigation software. As PET images have low spatial resolution, they should be combined with anatomic CT or MRI data sets for interpretation. We found this metabolic information of the tumor was particularly useful in patients with previous surgery and radiotherapy because it helped us differentiate tumor from scar tissue or postradiotherapy changes on anatomic imaging data sets (Patients 10 and 13) [14, 19]. This detailed and interactive image analysis was particularly helpful in difficult pelvic, sacral, or joint-saving bone tumor resections; the spatial relation of the tumor to nearby neural and vascular structures was seen better with the 3-D bone-tumor model. Surgical planning on the fused images could be transferred and performed under navigation guidance if the image preparation was performed with the same navigation system. We found the fusion images valuable for surgical planning in all our

patients as they provided better intraosseous and extraosseous extent of the tumors.

We are unaware of any reports asking whether surgeons could reproduce an intended resection of musculoskeletal bone tumors. Merging of postoperative with preoperative images and precise fitting of custom tumor prostheses might allow validation of the accuracy of a resection as planned. Our results suggest surgeons should be able to reproduce an intended resection reliably using a surgical navigation system. For Patients 5, 7, and 9 who had joint-saving intercalated resection after neoadjuvant chemotherapy, only 1.5 to 2 cm of the distal femoral epiphyses could be retained. Thus, even a small deviation from the planned resection would have compromised the precise fit and distal fixation of the custom joint-saving prostheses used in the reconstructions. Surgical navigation after image fusion made it possible for us to resect the bone exactly as planned in length and orientation, yielding a perfect match between the residual bone and the custom prostheses junctions. Studies have described using anatomic landmarks and correlating with measurements on preoperative MR images to define bone resection [5, 11]. However, that technique relies on 2-D measurements and may result in errors between the perceived anatomy and that seen during actual surgery.

In Patients 4 and 8 with an S2 schwannoma and a sacrum giant cell tumor (S2 and below) respectively, the tumors involved mainly the anterior bony structure of the sacrum rather than posterior structure. Image fusion when combined with surgical navigation allowed us to precisely mark the extent of the posterior bone window just enough to remove the tumor via one posterior approach. Thus we avoided unnecessary bony resection in a critical area without compromising oncologic principles.

Although the CT-based navigation system in this study originally was designed for spine surgery, accurate image-to-patient registration could be achieved in our patients with tumors involving pelvis and long bones. In image-guided craniomaxillofacial surgery, accurate and direct image-to-patient registration on MRI data sets can be achieved using the laser surface scanning technique [10, 13]. This technique, however, cannot be used in musculoskeletal tumor surgery. Thin 1- to 2-mm thick MR slices, which are necessary for accurate registration, are difficult to obtain in musculoskeletal bone tumors because the tumor dimensions often are quite large and there can be movement artifacts generated during the long scanning times. Magnetic resonance imaging data sets thus are not used routinely in computer-assisted orthopaedic surgery. The overall accuracy of computer navigation-assisted bone tumor surgery depends on the quality of the image fusion and accuracy of image-to-patient registration [15]. The accuracy of image fusion in turn depends on the quality of raw data images and is not able to outreach the resolution



of primary data sets. The navigation system is only as good as the raw data. Therefore, the time between imaging and surgery must be short to avoid a discrepancy resulting from changes in tumor size. We anticipate with the advent of a newer generation of CT and MRI scanners, image resolution will increase and will enable more accurate anatomic visualization.

Our study suggests it is technically feasible to integrate all anatomic and functional data to facilitate 3-D surgical planning in musculoskeletal bone tumors. This integrated image data set, when combined with surgical navigation, enabled us to reliably perform planned tumor resections, and it may offer clinical benefits. As technology is evolving, more precise and faster navigation software will be available for this new image processing technique in computer navigation-assisted tumor surgery.

**Acknowledgments** We thank Eric Wai-kin Ng and Keith Kam-shing Lee (ACAOS-ITAV team, Department of Orthopaedics and Traumatology, Prince of Wales Hospital, Hong Kong), for setup of the navigation system and documentation of operative procedures; Ulrich G. Buehner and Dr. Sarvestani Amir (R&D, Computer Assisted Applications, Stryker Navigation, Freiburg, Germany) for their support with use of the cranial navigation software; and Dr. Paul Unwin and the design team (Stanmore Implants Worldwide Ltd, Centre for Biomedical Engineering, Royal National Orthopaedic Hospital, Middlesex, UK) for the CAD custom tumor prosthesis. We also appreciate the assistance of Prof. Martin C. M. Wong and Man-ho Lee (Department of Rapid Prototyping & Tooling Unit, Hong Kong Polytechnic University) in use of the CAD software.

## References

- Anderson KC, Buehler KC, Markel DC. Computer assisted navigation in total knee arthroplasty: comparison with conventional methods. *J Arthroplasty*. 2005;20(7 suppl 3):132–138.
- Enneking WF, Dunham W, Gebhardt MC, Malawar M, Pritchard DJ. A system for the functional evaluation of reconstructive procedures after surgical treatment of tumors of the musculoskeletal system. *Clin Orthop Relat Res*. 1993;286:241–246.
- Gebhard F, Weidner A, Liener UC, Stockle U, Arand M. Navigation at the spine. *Injury*. 2004;35(suppl 1):S-A35–45.
- Grutzner PA, Suhm N. Computer aided long bone fracture treatment. *Injury*. 2004;35(suppl 1):S-A57–64.
- Gupta A, Pollock R, Cannon SR, Briggs TW, Skinner J, Blunn G. A knee-sparing distal femoral endoprosthesis using hydroxyapatite-coated extracortical plates: preliminary results. *J Bone Joint Surg Br*. 2006;88:1367–1372.
- Hufner T, Kfuri M Jr, Galanski M, Bastian L, Loss M, Pohlemann T, Krettek C. New indications for computer-assisted surgery: tumor resection in the pelvis. *Clin Orthop Relat Res*. 2004;426:219–225.
- Krettek C, Geerling J, Bastian L, Citak M, Rucker F, Kendoff D, Hufner T. Computer aided tumor resection in the pelvis. *Injury*. 2004;35(suppl 1):S-A79–83.
- Laine T, Lund T, Ylikoski M, Lohikoski J, Schlenzka D. Accuracy of pedicle screw insertion with and without computer assistance: a randomised controlled clinical study in 100 consecutive patients. *Eur Spine J*. 2000;9:235–240.
- Leong JL, Batra PS, Citardi MJ. CT-MR image fusion for the management of skull base lesions. *Otolaryngol Head Neck Surg*. 2006;134:868–876.
- Marmulla R, Hassfeld S, Lüth T, Mühling J. Laser-scan-based navigation in craniomaxillofacial surgery. *J Craniomaxillofac Surg*. 2003;31:267–277.
- Muscolo DL, Ayerza MA, Aponte-Tinao LA, Ranalletta M. Partial epiphyseal preservation and intercalary allograft reconstruction in high-grade metaphyseal osteosarcoma of the knee. *J Bone Joint Surg Am*. 2005;87(suppl 1, pt 2):226–236.
- Nemec SF, Donat MA, Mehrain S, Friedrich K, Krestan C, Matula C, Imhof H, Czerny C. CT-MR image fusion for computer assisted navigated neurosurgery of temporal bone tumors. *Eur J Radiol*. 2007;62:192–198.
- Raabe A, Krishnan R, Wolff R, Hermann E, Zimmerman M, Seifert V. Laser surface scanning for patient registration in intracranial image-guided surgery. *Neurosurgery*. 2002;50:797–801; discussion 802–803.
- Rege SD, Chaiken L, Hoh CK, Choi Y, Lufkin R, Anzai Y, Juillard G, Maddahi J, Phelps ME, Hawkins RA. Change induced by radiation therapy in FDG uptake in normal and malignant structures of the head and neck: quantitation with PET. *Radiology*. 1993;189:807–812.
- Sure U, Alberti O, Petermeyer M, Becker R, Bertalanffy H. Advanced image-guided skull base surgery. *Surg Neurol*. 2000;53:563–572; discussion 572.
- Wixson RL, MacDonald MA. Total hip arthroplasty through a minimal posterior approach using imageless computer-assisted hip navigation. *J Arthroplasty*. 2005;20(7 suppl 3):51–56.
- Wong KC, Kumta SM, Chiu KH, Antonio GE, Unwin P, Leung KS. Precision tumour resection and reconstruction using image-guided computer navigation. *J Bone Joint Surg Br*. 2007;89:943–947.
- Wong KC, Kumta SM, Chiu KH, Cheung KW, Leung KS, Unwin P, Wong MC. Computer assisted pelvic tumor resection and reconstruction with a custom-made prosthesis using an innovative adaptation and its validation. *Comput Aided Surg*. 2007;12:225–232.
- Wong WL, Hussain K, Chevretton E, Hawkes DJ, Baddeley H, Maisey M, McGurk M. Validation and clinical application of computer-combined computed tomography and PET with 2-[18F]-fluoro-2-deoxy-D-glucose head and neck images. *Am J Surg*. 1996;172:628–632.